Journal of the European Ceramic Society 17 (1997) 49–53

PII: S0955-2219(96)00071-4
0955-2219/97/$17.00

Recovery of Hysteresis Capacitance–Voltage Curves of MOS Capacitors Passivated with Bubbled Fluoride-Containing Glasses

Keiji Kobayashi

Toshiba ULSI Research Center, 1-Komukai, Toshiba-chi, Kawasaki, Japan

(Received 8 February 1996; revised version received 18 March 1996; accepted 28 March 1996)

Abstract

The capacitance and voltage (C–V) characteristics of metal, oxide and silicon (MOS) capacitors passivated by bubbled PbF_2–BaF_2–SiO_2–B_2O_3–GeO_2 glasses with various water and fluoride contents were investigated. As the OH^- absorption coefficients of the glass increased, adverse effects on the recovery of hysteresis loops of C–V curve shifts were observed. The water content is closely related to the fluoride content in these glasses. A bubbling technique for blowing dry air through the molten glass liquid during melting was effective for removal of the OH absorption band in the fluoride-containing glasses. The viscous flow point of the glass decreased with increasing degree of ionic character obtained from Hannay's equation. © 1996 Elsevier Science Limited.

1 Introduction

Borophosphosilicate glass films formed from inorganic gas sources have been widely used in high-density integrated circuits as dielectric insulators.[1–3] The advantageous properties of such films are conformal step coverage, effective protection against alkali ions, and fairly low reflow temperature. Highly doped borophosphosilicate glasses reflow at low temperatures to give step coverage of ultra-high-density integrated circuits, but they also suffer from a tendency to crystallize during the reflow process.[4] Such crystallization is a serious drawback in the planarization of ultra-high-density integrated circuits.[4]

It has been found that zinc borosilicate glasses have even lower flow temperatures than borophosphosilicate glasses, and they do not suffer from this problem of crystallite formation during the reflow process.[5,6] However, both borophosphosilicate and zinc borosilicate glasses contain small amounts of water,[7,8] and this adversely affects the capacitance and voltage (C–V) characteristics of MOS devices if they are rapidly heated. Past studies have shown that the abnormal C–V curves of MOS capacitors are a result of highly polarizable ions and OH^- radicals in the glass.[8,9]

In this paper, we discuss the relationship between OH^- radical absorption and shifts in the C–V curve for MOS capacitors passivated using non-crystallizable bubbled PbF_2–BaF_2–SiO_2–B_2O_3–GeO_2 glasses with ionic bonds, and investigate the application of these glasses to MOS capacitors.

2 Experimental

PbF_2–BaF_2–SiO_2–B_2O_3-GeO_2 glasses were prepared for use in the experiments. Batches comprising 1 kg of reagent-grade chemicals were melted at 1300°C for 5 h in an ultra-high-purity platinum crucible with an electric furnace in an oxidizing atmosphere. Dry air was blown for 1 h through liquid glass during melting in an oxidizing atmosphere using a platinum tube. This is the dry air bubbling technique.[7] After homogeneous melting, the glass was poured onto a stainless steel plate and annealed. Infra-red transmission spectra were measured using a Digi-Labo spectrophotometer with 10 mm × 20 mm × 1 mm plates. Glass flow points were obtained from thermal expansion curves, using a method previously described.[10]

Sputter targets were cut from these samples and ground to 75 mm in diameter and 10 mm thick. Glass films 0·5 μm thick were deposited on an SiO_2 layer (0·3 μm) on Si (100) wafers under 1 kW power and 4 MPa vacuum sputtering conditions using a Perkin–Elmer vacuum system. The glass thickness was measured by the use of a Nanometrics SD9-2000T thickness meter using the

Na-D line refractive index (N_D = 1·56). Aluminium electrodes were deposited on the glass films. C–V curves for these MOS capacitors were observed at 1 MHz at room temperature, as described previously.[11]

3 Results and Discussion

Low-temperature glass reflow has been studied and used in the planarization of MOS devices and the fabrication of multi-level interconnections.[5,6] It is thought that glass reflow is controlled by viscosity, which is in turn controlled by composition, chemical bond[12] and structure.[13,14] Namely, glass with 'low connectivity'[12] and 'a released structure'[13] is less viscous than that without such properties. It is to be expected that ionic bonds would give rise to a greater degree of viscous flow than covalent bonds. Pauling, and Hannay and Smyth[15] have proposed experimental equations for ionic bonding.

Pauling's equation and Hannay's equation were compared in the case of the application to the ionic character of fluoride-containing glasses, and Hannay's equation was found to be more reasonable than Pauling's equation in terms of the accuracy of the relation between flow points and the ionic bonding degree of glasses. Hannay and Smyth[15] proposed an experimental equation for ionic bonding as follows:

$$\text{Degree of ionic character (\%)} \quad I_i = 16\,(x_A - x_B) + 3{\cdot}5\,(x_A - x_B)^2 = (x_A - x_B)\,[16 + 3{\cdot}5\,(x_A - x_B)] \qquad (1)$$

where $(x_A - x_B)$ is the electronegativity difference for a bond A–B ($x_A > x_B$). The ionic character of a glass, I(%), can be described approximately as follows:

$$I = \Sigma I_i M_i \qquad (2)$$

where I_i is the ionic character of a single bond A–B making up the glass and M_i is the mole percentage of the ions making up the glass.

The author estimated the ionic character of glasses, using eqns (1) and (2). The chemical composition (mol%) of various glasses, their absorption coefficients (β_{OH}), ionic character, flow points (T_f), and C–V curve shift (ΔV_G) are listed in Tables 1 and 2, where the errors of β_{OH} values computed by eqn (5) are within ± 0·01 cm^{-1} and those of ΔV_G values measured are ± 0·1 V. Infra-red absorption spectra for these glasses are given in Figs 1 and 2. The absorption bands around 3500 cm^{-1} are due to fundamental vibrations arising from OH ion absorption.[16–18]

The relationship between transmittance T_{OH} and reflectivity R_{OH} can be represented as follows:[18]

$$T_{OH} = 1 - [R_{OH}(1 - R_{OH}) + R_{OH}] = (1 - R_{OH})^2 \qquad (3)$$

The absorption coefficient β_{OH} resulting from the fundamental vibration due to OH at around 3500 cm^{-1} is calculated from:[19]

$$T_{OH} = [(1 - R_{OH})^2\, e^{-\beta_{OH} t}]/[1 - R_{OH}^2 e^{-2\beta_{OH} t}] \qquad (4)$$

where t is the glass thickness.

By substituting eqn (3), eqn (4) can be simplified as follows:

$$e^{-\beta_{OH} t} + R_{OH}^2 e^{-2\beta_{OH} t} = 1 \qquad (5)$$

Values of OH^- absorption coefficients β_{OH} are computed from eqn (5). Values of T_{OH}, R_{OH} and β_{OH} calculated from the infra-red absorption spectra in Figs 1 and 2 are also listed in Table 1 and 2. Infra-red absorption spectra of these glasses are

Table 1. List of glass compositions, T_{OH}, R_{OH}, β_{OH}, T_f, I and ΔV_G. Glasses no. (1)–(5) are without bubbling

Glass no.	PbF_2 *(mol%)*	BaF_2 *(mol%)*	SiO_2 *(mol%)*	B_2O_3 *(mol%)*	GeO_2 *(mol%)*	T_{OH} *(%)*	R_{OH}	β_{OH} *(cm^{-1})*	I *(%)*	T_f *(°C)*	ΔV_G *(V)*
(1)	2	1	27	50	20	50	0·29	0·74	35·2	770	2·5
(2)	4	2	24	50	20	55	0·26	0·61	35·9	765	2·0
(3)	6	3	21	50	20	62	0·21	0·41	36·5	763	2·0
(4)	8	4	18	50	20	67	0·14	0·28	37·2	756	1·5
(5)	10	5	15	50	20	70	0·16	0·26	37·9	745	1·0

Table 2. List of T_{OH}, R_{OH}, β_{OH}, I, T_f, I and ΔV_G. Glasses from (6) to (10) are dry-air bubbled: (6) glass no. (1) bubbled, (7) glass no. (2) bubbled, (8) glass no. (3) bubbled, (9) glass no. (4) bubbled; (10) glass no. (5) bubbled.

Glass no	T_{OH} *(%)*	R_{OH}	β_{OH} *(cm^{-1})*	I *(%)*	T_f *(°C)*	ΔV_G *(V)*
(6)	65	0·19	0·36	35·2	773	1·5
(7)	68	0·18	0·30	35·9	767	1·4
(8)	70	0·16	0·26	36·5	765	1·2
(9)	73	0·15	0·20	37·2	757	1·0
(10)	76	0·13	0·16	37·9	746	0·8

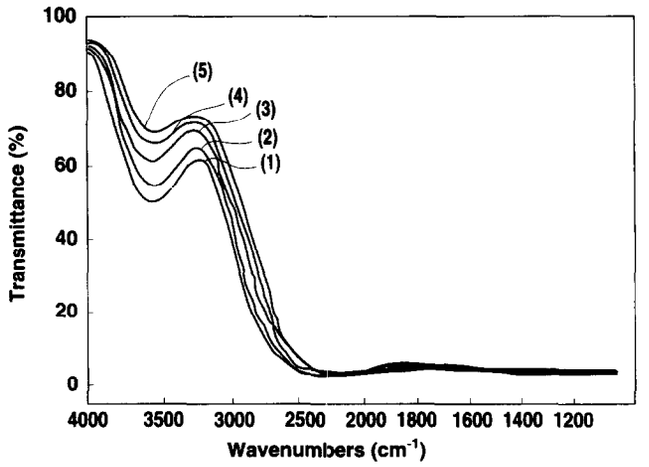

Fig. 1. Infra-red absorption spectra for PbF_2–BaF_2–SiO_2–B_2O_3–GeO_2 glasses without bubbling. (1) glass no. (1), (2) glass no. (2), (3) glass no. (3), (4) glass no. (4), (5) glass no (5).

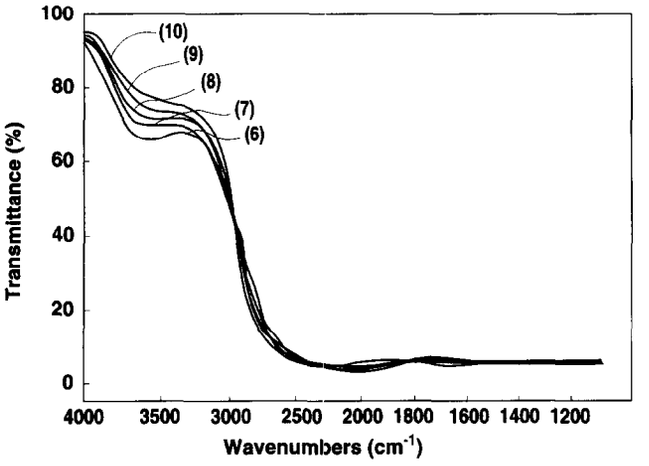

Fig. 2. Infra-red absorption spectra for dry-air bubbled PbF_2–BaF_2–SiO_2-B_2O_3–GeO_2 glasses. (6) Glass No. (1), (7) glass no. (2), (8) glass no. (3), (9) glass no. (4), (10) glass no. (5).

given in Figs 1 and 2, which shows the decrease of OH absorption bands with the increase of fluoride content in the glasses. Fluoride compounds react with water in the batch during melting, as represented in the following equation:

$$RF_2 + H_2O \rightarrow RO + 2HF\uparrow \qquad (6)$$

where R = Ba, Pb. Consequently, the reaction of water with fluoride groups in glasses would be advantageous as a means of improving their infra-red absorption transmissions in the region of the water peaks. Furthermore, the dry air bubbling technique is effective for the removal of OH bands in glasses, as shown in Fig. 2.

Thermal expansion curves of PbF_2–BaF_2–SiO_2–B_2O_3–GeO_2 glasses are given in Figs 3 and 4, which also show the glass flow points. Flow points fell with increasing ionic character in the chemical bonds. This tendency is clear in Table 1. With regard to the *C–V* curve shifts in MOS capacitors, when OH absorption coefficients increased, ΔV_G

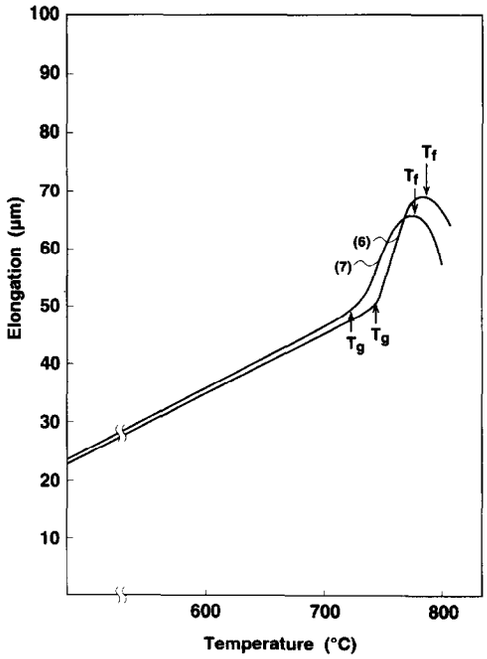

Fig. 3. Thermal expansion curves for dry-air bubbled PbF_2–BaF_2–SiO_2–B_2O_3–GeO_2 glasses. (6) Glass no. (1), (7) glass no. (2).

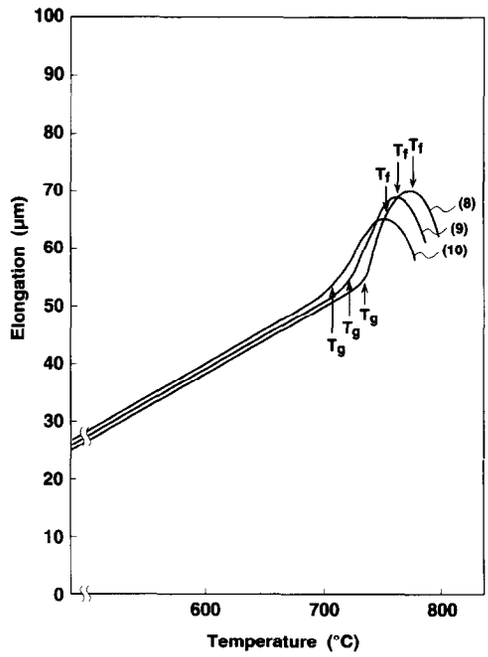

Fig. 4. Thermal expansion curves for dry-air bubbled PbF_2–BaF_2–SiO_2–B_2O_3–GeO_2 glasses. (8) Glass no. (3), (9) glass no. (4), (10) glass no. (5).

shifts also increased. The *C–V* characteristics of MOS capacitors passivated with these glasses are shown in Figs 5 and 6. As can be seen, all the *C–V* curves for capacitors passivated with these glasses shifted towards the right. Thus, these peculiar *C–V* characteristics represent the recovery of *C–V* curve shifts as the coefficients of OH absorption decrease. With increasing β_{OH}, the *C–V* curves shift towards the right. The mean *C-V* curve shifts, ΔV_G, at the mid point of front and back hysteresis curves are summarized in Table 1 and 2.

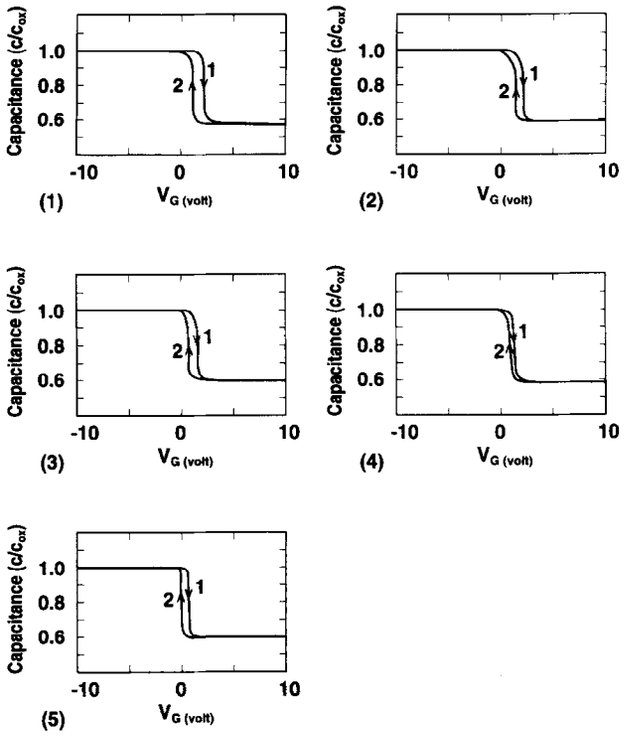

Fig. 5. C–V curve characteristics of thermally annealed MOS capacitors passivated by PbF_2–BaF_2–SiO_2–B_2O_3–GeO_2 glasses without bubbling. 1 is a front curve, 2 is a back curve. (1) Glass no. (1), (2) glass no. (2), (3) glass no. (3), (4) glass no. (4), (5) glass no. (5).

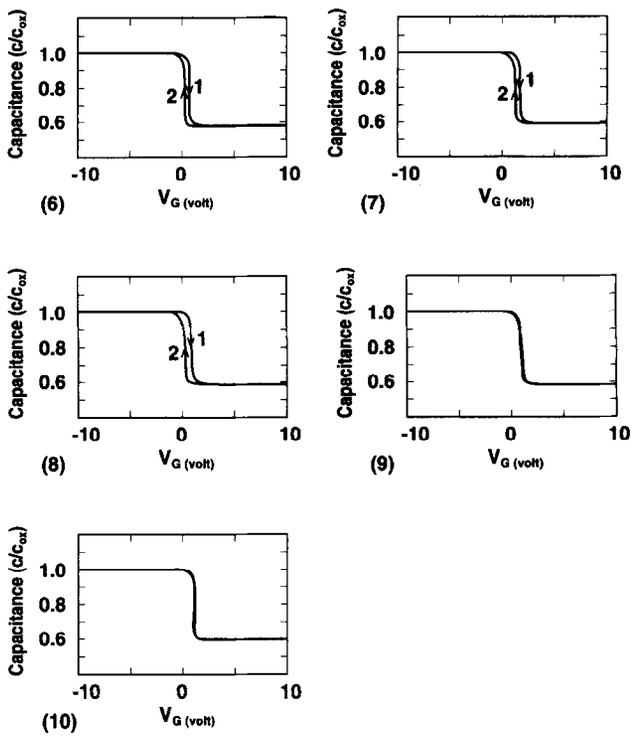

Fig. 6. C–V curve characteristics of thermally annealed MOS capacitors passivated by dry-air bubbled PbF_2–BaF_2–SiO_2–B_2O_3–GeO_2 glasses. (6) Glass no. (1), (7) glass no (2), (8) glass no. (3), (9) glass no. (4), (10) glass no. (5).

The hysteresis curves for these MOS capacitors also showed good reproducible capability as required for the MOS device passivations. These shifts in the C–V curves indicate that the total number of positive oxide charges increases. It is reasonable to expect that these positive charges are hydrogen-related vacancies.[9] The loss of hydrogenous species is related to the disappearance of C-V hysteresis. A hydrogenous complex is responsible for the carrier trapping mechanism.[9] These shifts are related to hydrogen-related vacancies in water-containing glasses.[9]

4 Conclusion

When the viscous flow point of these glasses became higher, the degree of ionic bonding character was reduced and the OH absorption coefficient was raised. This tendency may be due to fluoride contents in molten glasses. The viscous flow is reasonably confirmed from the ionic character of bonding state as calculated from Hannay's experimental equation.

The MOS capacitors passivated with PbF_2–BaF_2–SiO_2–B_2O_3–GeO_2 glasses containing low concentrations of water exhibited the best recovery in their C–V characteristics. With increasing OH absorption coefficient, an adverse effect was seen on the recovery of hysteresis C–V curve shifts. Moreover, the dry air bubbling technique was effective for the removal of OH bands. Hysteresis and V_G shifts for MOS capacitors passivated with bubbled fluoride-containing glasses were improved using the technique. Particularly, a few MOS capacitors showed no hysteresis curve. After the heating, the recovery of hysteresis and ΔV_G shifts for these MOS capacitors showed good reproducible capability as required for MOS device passivations. The relationship between recovery from the peculiar hysteresis C–V curve shifts and OH absorption coefficient was briefly discussed.

Acknowledgement

The author would like to thank Dr H. Sasaki in Toshiba Research and Development Center for the measurement of infra-red absorption spectra.

References

1. Hurley, K. H., *Solid St. Technol.*, March (1987) 103.
2. Dickinson Jr, J. E. & deJong, B. H. W. S., *J. Non-cryst. Solids*, **102** (1988) 196.
3. Raley, N. F. & Losee, D. L., *J. Electrochem. Soc.*, **135** (1988) 2640.
4. Schnable, G. L., Fisher, A. W. & Shaw, J. M., *J. Electrochem. Soc.*, **135** (1990) 3973.
5. Kobayashi, K., *J. Non-cryst. Solids*, **88** (1986) 229.

6. Kobayashi, K., *J. Non-cryst. Solids*, **167** (1994) 180.
7. Kobayashi, K., *J. Electrochem. Soc.*, **131** (1984) 2190.
8. Rojas. S., Gomarasca, R., Zanotti, A., Borghesi, A., Sassela, G., Ottaviani, L. M. & Lazzeri, P., *J. Vac. Sci. Technol. B*, **10** (1992) 633.
9. Li, S. C., Murarka, S. P., Guo, X. S. & Lanford, W. A., *J. Appl. Phys.*, **72** (1992) 2947.
10. Baret, G., Madar, R. & Bernar, C., *J. Electrochem. Soc.*, **138** (1991) 2835.
11. Kobayashi, K., *J. Non-cryst. Solids*, **124** (1990) 229.
12. Kobayashi, K., *J. Non-cryst. Solids*, **159** (1993) 274.
13. Kobayashi, K., *Glass Technol.*, **29** (1988) 253.
14. Kobayashi, K., *Glass Technol.*, **30** (1989) 110.
15. Hannay, N. B. & Smyth, C. P., *J. Am. Chem. Soc.*, **68** (1946) 171.
16. Shaw, C. M. & Shelby, J. E., *Phys. Chem. Glasses*, **34** (1993) 35.
17. Kobayashi, K., *Glass Technol.*, **34** (1993) 120.
18. Ruller, J. A. & Shelby, J. E., *Phys. Chem. Glasses*, **33** (1992) 177.
19. Zhenhua, L. & Frischat, G. H., *J. Nom-cryst. Solids*, **163** (1993) 169.